



OPEN ACCESS

Edited by:

Olivier Feron,
Université catholique de Louvain,
Belgium

Reviewed by:
Michael Orth,

LMU Munich University Hospital,
Germany
Urbain Weyemi,
University of Texas at Austin,
United States

***Correspondence:**

Robert A. Newman
newmanscientificconsulting@
gmail.com

Claudio Festuccia
Claudio.festuccia@univaq.it

[†]These authors share first authorship

Specialty section:

This article was submitted to
Pharmacology of Anti-Cancer Drugs,
a section of the journal
Frontiers in Pharmacology

Received: 11 January 2022

Accepted: 02 March 2022

Published: 23 March 2022

Citation:

Colapietro A, Yang P, Rossetti A, Mancini A, Vitale F, Chakraborty S, Martelluci S, Marampon F, Mattei V, Gravina GL, Iorio R, Newman RA and Festuccia C (2022) The Botanical Drug PBI-05204, a Supercritical CO₂ Extract of *Nerium Oleander*, Is Synergistic With Radiotherapy in Models of Human Glioblastoma. *Front. Pharmacol.* 13:852941.
doi: 10.3389/fphar.2022.852941

The Botanical Drug PBI-05204, a Supercritical CO₂ Extract of *Nerium Oleander*, Is Synergistic With Radiotherapy in Models of Human Glioblastoma

Alessandro Colapietro ^{1†}, Peiying Yang ^{2†}, Alessandra Rossetti ¹, Andrea Mancini ¹, Flora Vitale ³, Sharmistha Chakraborty ², Stefano Martelluci ^{4,5}, Francesco Marampon ⁶, Vincenzo Mattei ⁴, Giovanni Luca Gravina ^{1,7}, Roberto Iorio ⁸, Robert A. Newman ^{9*} and Claudio Festuccia ^{1*}

¹Laboratory of Radiobiology, Department of Biotechnological and Applied Clinical Sciences, University of L'Aquila, L'Aquila, Italy,

²Department of Palliative, Rehabilitation and Integrative Medicine, The University of Texas MD Anderson Cancer Center, Houston, TX, United States, ³Laboratory of Neurophysiology, Department of Biotechnological and Applied Clinical Sciences, University of L'Aquila, L'Aquila, Italy, ⁴Biomedicine and Advanced Technologies Rieti Center, Sabina Universitas, Rieti, Italy, ⁵Laboratory of Experimental Medicine and Environmental Pathology, University Hub "Sabina Universitas", Rieti, Italy, ⁶Department of Radiological, Oncological and Pathological Sciences, Sapienza University of Rome, Rome, Italy, ⁷Division of Radiation Oncology, Department of Biotechnological and Applied Clinical Sciences, University of L'Aquila, L'Aquila, Italy, ⁸Laboratory of Biology, Department of Biotechnological and Applied Clinical Sciences, University of L'Aquila, L'Aquila, Italy, ⁹Phoenix Biotechnology, Inc., San Antonio, TX, United States

Glioblastoma multiforme (GBM) is the most common as well as one of the most malignant types of brain cancer. Despite progress in development of novel therapies for the treatment of GBM, it remains largely incurable with a poor prognosis and a very low life expectancy. Recent studies have shown that oleandrin, a unique cardiac glycoside from *Nerium oleander*, as well as a defined extract (PBI-05204) that contains this molecule, inhibit growth of human glioblastoma, and modulate glioblastoma patient-derived stem cell-renewal properties. Here we demonstrate that PBI-05204 treatment leads to an increase *in vitro* in the sensitivity of GBM cells to radiation in which the main mechanisms are the transition from autophagy to apoptosis, enhanced DNA damage and reduced DNA repair after radiotherapy (RT) administration. The combination of PBI-05204 with RT was associated with reduced tumor progression evidenced by both subcutaneous as well as orthotopic implanted GBM tumors. Collectively, these results reveal that PBI-05204 enhances antitumor activity of RT in preclinical/murine models of human GBM. Given the fact that PBI-05204 has already been examined in Phase I and II clinical trials for cancer patients, its efficacy when combined with standard-of-care radiotherapy regimens in GBM should be explored.

Keywords: glioblastoma, radiotherapy, PBI-05204, apoptosis, oleandrin, DNA repair

INTRODUCTION

Glioblastoma multiforme (GBM) is a stage IV glioma based on WHO grading criteria and is the most common primary brain tumor with a 5-year survival rate close to 7.2% (Wu et al., 2021). Surgery is the primary form of treatment but, unfortunately, it is rarely curative. These tumors invade healthy brain tissue at a microscopic level, not allowing complete resection therefore resulting in disease recurrence. For this reason, surgical resection of tumor tissue is followed by radiotherapy and/or chemotherapy (Stupp et al., 2009). Radio- and chemo-resistance are widely involved in the recurrence from treated GBM and represent major obstacles to successful treatment. The robust DNA repair and self-renewing capabilities of GBM cells and glioma stem or infiltrating cells promote resistance against current treatment modalities (Haque et al., 2011). Failure of standard of care chemo/radiotherapy regimens has been attributed to multiple factors, such as microenvironment protection, *de novo* and/or acquired tumor resistance, limitations in drug delivery, increased angiogenesis and/or vasculogenic mimicry (VM), and presence of glioma stem cells (GSCs) (Auffinger et al., 2015). Due to the poor prognosis of high-grade glial tumors, exploration and development of novel treatment strategies remains an essential need.

Both PBI-05204 and its active principal ingredient, oleandrin, have been tested in GBM models (Colapietro et al., 2020a) and, in addition, have also been shown to be active against a wide number of human tumor cell types such as melanoma (Lin et al., 2008), prostate (Smith et al., 2001), pancreas (Pan et al., 2015), and breast (Li et al., 2021) cancers as well as certain hematologic malignancies. The botanical drug PBI-05204 has gone through both Phase I and II clinical trials in cancer patients and has been shown to be safe as an oral drug for daily administration (Hong et al., 2014; Roth et al., 2020). It has been reported that oleandrin inhibits activation of NF- κ B (Kanwal et al., 2020) with repercussions on metabolic arrest as a defense strategy against hypoxia and recruitment of cancer stem cells after cellular stress caused by pharmacological and therapeutic approaches. In addition to its suppressive effect in tumor cell proliferation, oleandrin as well as other cardiac glycosides have been reported to enhance the *in vitro* radiosensitivity of human NSCLC A549 (Lawrence, 1988) and prostate cancer PC3 cells (Nasu et al., 2002). The radiosensitizing effect of oleandrin was mediated by activation of caspase 3 associated apoptotic pathways (Nasu et al., 2002). The potential mechanisms associated with radiosensitization include inhibition of repair of radiation-induced damage, changes in tumor cell prosurvival signaling pathways, induction of programmed cell death, and/or changes in cellular metabolism, and reduction of cancer cell stemness (Wang et al., 2018). The stem cell component plays an important role in GBM pathology because on the one hand this gives rise to new cancer cells ready to differentiate and on the other hand leads to new cancer stem cells, capable of supporting progression and tumor survival, and therefore, of maintaining a pool of residual cancer stem cells (Vlashi and Pajonk, 2015; Liu et al., 2020; Mattei et al., 2021). Moreover, this stem cell component provides the means by which tumors acquire resistance to standard of care

radio- and chemotherapeutic treatments (Lathia et al., 2015). All of which suggests that to be a highly effective therapy against GBM, an agent should have a multifaceted capability of inhibiting tumor growth. This would include the ability to enhance radiation mediated inhibition of tumor cell proliferation, possess several demonstrated anticancer effects that are in some cases distinct from conventional chemotherapeutic agents and, finally, it should also demonstrate an ability to inhibit GBM stem cell activation to assist with inhibition of tumor regrowth.

Our previous study has reported the anti-tumor effects of PBI-05204 on GBM cells (Colapietro et al., 2020a). Subcutaneous and orthotopic intra-brain xenografts also revealed that PBI-05204 showed important *in vivo* effects evidenced by reduced tumor progression and increased disease free survival as well as enhanced overall survival. In the current study, we have examined the possibility that PBI-05204 may have significant sensitizing effects on radiotherapy. This has been explored using *in vitro* studies of human GBM cell proliferation as well as *in vivo* human tumor growth in immunocompromised mice. Importantly, studies of proposed mechanisms of enhanced interaction with radiotherapy including DNA damage and repair are presented as well as effects on glioblastoma stem cell proliferation.

MATERIAL AND METHODS

Cell Lines and Cell Cultures

Materials for tissue culture were purchased from the Italian distributor of Euroclone (Euroclone S.p.A, Milan, Italy). Four human glioma cell lines (U251, A172, U87MG and T98G) were cultured at 37°C in 5% CO₂ in Dulbecco's modified Eagle medium (DMEM) containing 10% (v/v) fetal bovine serum, 4 mM glutamine, 100 IU/ml penicillin, 100 µg/ml streptomycin and 1% nonessential amino acids (Thermo Fisher Scientific Inc., Carlsbad, CA, United States). The risk of working with misidentified and/or contaminated cell lines was minimized by using GBM cells at very low passages and performing periodic short tandem repeat (STR) DNA profiling. Luciferase tagged U87MG cells were generated and provided by Jari E. Heikkila (Abo Akademi University, Turku, Finland). Isolated neurospheres were assayed for stemness properties in terms of clonogenic capacity and positivity for stem cell markers.

Reagents

Antibodies against γH2AX (STJ90288), Ku70 (STJ29469), pDNA-PKc (STJ91334), caspase 3 (STJ11101177), cleaved caspase 3 (STJ90005), caspase 9 (STJ29774), cleaved caspase 9 (STJ90013), LC3A/LC3B (STJ117779) were purchased from St John's Laboratory Ltd. (Knowledge Dock Business Centre Docklands Campus, London, United Kingdom). Antibodies against DNA-PKc (clone G-4: sc-5282), Rad51 (clone F-11: sc-398587), p62 (clone D3, sc-28359), OCT3/4 (C-10, sc-5279), and βIII tubulin (clone 3H3091, sc-69966) were purchased from Santa Cruz Biotechnology (Santa Cruz, CA, United States). Antibody against Ki67 (Clone MIB-1, M7240) was purchased from Dako

(Agilent Technologies Italia S.p.A., Cernusco sul Naviglio, Milan, Italy). Antibodies against CD44 (ab157107) and Stro-1 (ab214086) were purchased from Abcam (Cambridge, United Kingdom).

Immunofluorescence Studies

Glioma stem like cells were used for immuno-fluorescence analyses. Spheres were seeded at a density of 10,000 cells/cm² on glass coverslips pretreated with 30 µg/ml Poly-L lysine to promote adherence. The slides were then washed twice with phosphate-buffered saline (PBS) and fixed with 4% paraformaldehyde for 20 min at room temperature. To stain cytoplasmic markers, slides were permeabilized with 0.3% Triton-X-100 for 5 min at room temperature. Spheres were then incubated overnight at 4°C with the following primary antibodies accordingly to their data sheets: anti-OCT3/4 and anti-SOX2. After washing with PBS, cells were incubated for 30 min at room temperature with AlexaFluor 488 anti-rabbit IgG, AlexaFluor 595 anti-goat IgG or AlexaFluor 633 anti-mouse IgG secondary antibody (1:2000; Molecular Probes, Invitrogen, Carlsbad, CA, United States). Controls were performed by omitting the primary antibody. Cell nuclei were stained with DAPI (0.5 µg/ml). Coverslips were mounted with Vectashield Mounting Medium and examined with a Leica TCS SP5 confocal microscope (Leica Microsystems Inc., Mannheim, Germany).

U251 and U87MG GBM cells were seeded at a density of 10,000 cells/cm² on glass coverslips pretreated with 30 µg/ml Poly-L lysine to promote adherence. The slides were then washed twice with phosphate-buffered saline (PBS) and fixed with a mixture of cold methanol:acetone (1:1) for 5 min. Immunofluorescence for γH2Ax was then performed by incubating the cells with primary γH2Ax antibody (1:50) for 1 h at room temperature. After extensive washing in PBS, a secondary antibody was incubated for 30 min. After washing, nuclei were counterstained with DAPI and staining was analyzed as described above.

Acidic Vesicular Organelle (AVO) Staining

In order to quantify the change in the number of AVOs in cells treated with PBI-05204 and/or RT, cells were stained with Acridine Orange (1 µg/ml) in PBS at 37°C for 15 min in the dark. The cells were then washed with PBS twice and suspended in PBS for immediate analysis. Cells were analyzed with a Leica TCS SP5 confocal microscope (Leica Microsystems Inc., Mannheim, Germany). AVOs were quantified using Fiji/ImageJ software.

Fluorescence-Activated Cell Sorter (FACS) Analyses

Expression of surface antigens in Glioma stem like cells, treated or untreated with PBI-05204 at opportune doses was quantified by flow cytometry. Cells were fixed with 4% paraformaldehyde for 10 min at 4°C and, after washing, cells were incubated for 1 h at room temperature with anti-CD44, anti-stro-1, and Ki67 followed by an additional 30 min with CY5-conjugated anti-rabbit IgG H&L or PE-conjugated anti-mouse IgG purchased

from Abcam (Cambridge, United Kingdom). All samples were analyzed using a BD AccuriTM C6 Plus Flow cytometer (Becton Dickinson Italia SpA, Milan, Italy) equipped with a blue laser (488 nm) and a red laser (640 nm). At least 10,000 events were acquired. Negative controls were obtained by analyzing samples treated without the primary antibody.

Growth Assays and Viability

Twenty-four-well plates were seeded with 2 × 10⁴ GBM cells/well. After cell adhesion and growth in 5% fetal calf serum (FCS) DMEM for 24 h, different concentrations of PBI-05204 were added. A Nikon Diaphot inverted phase-contrast photomicroscope (Nikon Corp., Tokyo, Japan) was used before cell trypsinization and counting. Viable cell counts were made by an exclusion assay with use of a NucleoCounter NC-100 (Chemotec, Gydevang, Denmark) according to the manufacturer's instructions and as previously described (Gravina et al., 2016). IC₅₀ values, the concentrations of drugs required for a 50% reduction in growth/viability, were calculated using the Dojindo Cell Counting Kit-8 (Dojindo EU GmbH, Munich, Germany). For determination of relative neurosphere proliferation, two different modalities of study were used: 1) a direct count and sizing of neurospheres at 1 week of culture from pre-formed spheres, and 2) an evaluation of the clonal capacity of cancer stem cells (CSCs) cultured as single cells after 14–30 days. For analysis of sphere growth, preformed neurospheres were treated with RT alone or RT plus different doses of PBI-05204 for 72 h. After treatment, spheres were photographed and counted with a contrast phase microscope. Spheres were recorded as either large colonies (>20 cells) or small colonies (<20 cells). Single cells were also manually counted per microscopic field at ×100 magnification. For the clonogenic assay, glioma tumor-initiating cells (GICs) were seeded in 96-well plates as a single cell suspension at a density of 2 cells/ml. Cells were maintained for 14–30 days in media and then the wells were visually scanned by light microscopy to identify and count the clones (spheres) produced. Apoptosis was evaluated by APOSTRAND™ ELISA apoptosis detection kit (3V Chimica S.r.l. Rome, Italy) and caspase-specific chromogenic substrates at 450 nm in a microplate reader. Ac-DEVD-pNA (caspase-3) and Ac-IETD-pNA (caspase 9) were purchased from Kaneka Eurogentec SA (Seraing, Belgium).

Clonogenic Survival

Cells in culture were exposed to different concentrations of PBI-05204 for 24 h and in some experiments the cells were pretreated with an inhibitor of caspase-3, Z-DEVD-FMK (10.0 µM, 2 h) (Calbiochem, San Diego, CA, United States) or 3 methyl adenine (3 mM), an inductor of lysosomal self-degradation before PBI-05204 was added to the culture. Cells were then irradiated with doses of 2, 4 or 6 Gy of γ-rays using a ¹³⁷Cs source (3.7 Gy/min) and assayed for colony forming ability by replating them in specified numbers (1,000 cells) into 100-mm dishes containing drug-free media. After 12 or 30 days of incubation, cells were stained with 0.5% crystal violet in absolute ethanol, and colonies with >50 cells were counted (Gravina et al., 2014). Radiation survival curves were plotted after normalizing for cytotoxicity

induced by PBI-05204 alone. Clonogenic survival curves were constructed from at least three independent experiments. The survival curves were analyzed using MedCalc statistical software. The data were fitted by a weighted and stratified linear regression, according to the linear-quadratic formula: $S(D)/S(O) = \exp(-\alpha D + \beta D^2)$. The cell survival enhancement ratio (DER) was calculated as the ratio of the mean inactivation dose under control conditions divided by the mean inactivation dose after treatments exposure (Roeske et al., 2007; Granzotto et al., 2011; Petragnano et al., 2020).

Matrigel Invasion and Vasculogenic Mimicry Assays

Cell migration assays were carried out by allowing the cells to migrate through a protein mixture (Matrigel 50 ml of 25 mg/ml). Semi-permeable membrane cell culture inserts of polycarbonate with pores of 8 μm were inserted in the Boyden chambers and an aliquot of 200 μl of chemoattractant (3T3 conditioned media) was added to the lower chamber. Cells (8×10^5) were seeded on the top of each filter. Adhesion and successive migration were analyzed after 6 h of test in which untreated or treated cells (RT, PBI-05204 and combination RT + PBI-05204) were left to adhere and migrate. Non-adherent cells were removed from the upper portion of filters with a cotton swab. The migrated cells were stained with Diff-Quik, a commercial Romanowsky stain and then counted. For each filter, cells from five fields at $200\times$ (20×10) magnification were counted and cell counts from 15 fields were considered for statistical analyses.

Vasculogenic mimicry assays were performed by first placing Matrigel (200 μl) into 48-well tissue culture plates followed by incubation at 37°C for 24 h to allow adhesion and tube formation of GBM cells. Cells were pre-treated with RT, PBI-05204 or RT plus PBI-05204 for 24 h and seeded onto the coated plate at a concentration of 2×10^5 cells/ml. After 16 h incubation, tube formation was assessed using an inverted microscope and image J software to calculate the number of branches from tubules.

Western Blot Analyses

Cell extracts were obtained from treated or untreated cultures washed with cold PBS and lysed with lysis buffer containing proteinase and phosphatase inhibitor cocktails. Proteins were subjected to 7 or 15% sodium dodecyl sulphate-polyacrylamide gel electrophoresis (SDS-PAGE), transferred to nitrocellulose and probed with appropriate antibodies based on the recommendations of the suppliers. Reactive bands were visualized with a chemiluminescent detection kit (Perbio Science, Tattenhall, United Kingdom) in a Bio-Rad gel Doc system (Bio-Rad Laboratories S.r.l., Milan, Italy). Normalization of specific bands was performed using an anti β -actin or anti-tubulin antibody.

γ H2AX ELISA Assay

Levels of γ H2AX in the cell lysates were determined using Human Phospho-Histone H2AX (S139) DuoSet IC ELISA kit (# DYC2288-2; R&D Systems). ELISA was performed on total cell extracts derived from cells treated with PBI-05204, RT and PBI-05204 + RT.

After treatment at different time points, i.e. 1, 4, 8, 16, 24 and 48 h, cells were collected and subjected to protein extraction. An aliquot of 200 μl of lysis buffer (RIPA + inhibitors of proteases and phosphatases) was added to each well and cells were scraped. An additional 200 μl of lysis buffer was used to ensure collection of all cells. Cell suspensions were sonicated and centrifuged for 10 min (14,000 rpm) at 4°C and supernatants were transferred to new tubes. Cell lysates were stored at -80°C and ELISA was performed when the cell lysates from all the treatments at different time points had been collected.

Comet Assay

After treatments, 1×10^5 cells were digested, purified, and mixed with 30 μl of low-melting-point agarose (LMPA, 1% DMEM solution). This cell solution was then dropped on a glass slide to form a thin film and cooled for 10 min using ice to allow solidification. An additional 75 μl of LMPA (1% DMEM solution) was dropped on this glass slice as the top layer, and the process was repeated. These samples were dipped in the lysis solution (containing 10 mM Tris-HCl, 2.5 M NaCl, 100 mM Na₂EDTA, 1% Triton X-100) overnight. The DNA sample was unwound for 20 min in the alkaline electrophoresis solution and electrophoresis performed for 20 min (voltage 1 V/cm and current 300 mA). Finally, these samples were stained using ethidium bromide (EB; 100 μl , 20 $\mu\text{g}/\text{ml}$). The images of DNA damage were obtained using a Leica TCS SP5 confocal microscope (Leica Microsystems Inc., Mannheim, Germany). Images were collected in Black/White to have a higher resolution for analyses. Comets were analyzed by Comet Assay Software (CaspLab).

In Vivo Experiments: Xenograft Model

Female CD1-nu/nu mice, at 6 weeks of age, were purchased from Charles River (Milan, Italy) under the guidelines established by our Institution (University of L'Aquila, Medical School and Science and Technology School Board Regulations, complying with the Italian government regulation n.116 January 27, 1992 for the use of laboratory animals). All mice received subcutaneous flank injections (one each side) of 1×10^6 U251, U87MG or T98G cells. Tumor growth was assessed bi-weekly by measuring tumor diameters with a Vernier caliper. Xenografts were considered as equivalent to ovoids having three diameters: the formula used was 'TW (mg) = tumor volume (mm³) = 4/3 π R1xR2xR3 in which R1/R2/R3 are the 1/2 diameters (rays), shorter diameter is the thickness/height of tumor, larger diameters are the length and width of tumor (Colapietro et al., 2020a; Colapietro et al., 2020b). Thirty mice with tumor volumes of 0.8–1.3 cm³ were retained and randomly divided into four groups (five mice per group with two tumors each): 1) Control (vehicle); 2) RT (single 4 Gy dose at day 3); 3) PBI-05204 (20 mg/kg/5 Day/week, PO); 4) RT plus PBI-05204 (24 h of pre-treatment). At the end of experiments (35 days after the start of treatments) animals were sacrificed by carbon dioxide inhalation and tumors were subsequently removed surgically. The following parameters were used to quantify the antitumor effects upon different treatments as previously described (Gravina et al., 2017; Colapietro et al.,

2020a; Colapietro et al., 2020b): 1) Tumor volumes were measured during and at the end of experiments. 2) Tumor weights were measured at the end of experiments.

Orthotopic Intra-Brain Model

Female CD1 nu/nu mice were inoculated intra-cerebrally as previously described (Gravina et al., 2017; Colapietro et al., 2020a; Colapietro et al., 2020b) with luciferase transfected U87 cells. Prior to treatment initiation (5 days after injection), animals were randomized to control (vehicle), RT (4 Gy once), PBI-05204 (20 mg/kg, PO daily), and RT plus PBI-05204 groups ($n = 10$ each per group). Treatments were completed in 35 days. *In vivo* bioluminescence images were obtained weekly using the UVITEC Cambridge Mini HD6 (UVItec Limited, Cambridge, United Kingdom). Animals were anesthetized and luciferin (150 mg/kg) was injected intra-peritoneally (IP) 15 min prior to imaging. The mice were photographed while placed on their front and the bioluminescence intensity (BLI) was measured in the region of interest. We deliberately inoculated a small number of U87-Luc cells (3×10^3) to simulate a chemo-radio-therapeutic treatment made after surgery in which a low number of tumor cells, remaining in the wound bed, would re-grow resulting in a recurrence. Treatments were started 5 days after cell injection when no intracranially luciferase activity was detectable. Mice were euthanized when they displayed adverse neurological signs (e.g., altered gait, tremors/seizures, lethargy) or weight loss of 20% or greater relative to pre-surgical weight. The time at which a visible bioluminescence lesion was observed defined disease free survival (DFS). Overall survival (OS), defined as the time (days) prior to which an animal did not show the aforementioned distress signs, and was also determined.

Statistical Details

Continuous variables were summarized as mean and standard deviation (SD) or as median and 95% confidence intervals (CI). For continuous variables not normally distributed, statistical comparisons between control and treated groups were established by carrying out the Kruskal-Wallis test and Dwass-Steel-Chritchlow-Fligner method. For continuous variables normally distributed, statistical comparisons between control and treated groups were established by carrying out an analysis of variance (ANOVA) test or by Student t test for unpaired data (for two comparisons). When the ANOVA test revealed a statistical difference, pairwise comparisons were made by Tukey's honestly significant difference (HSD) test. TTP was analyzed by Kaplan-Meier curves and Gehan's generalized Wilcoxon test. When more than two survival curves were compared the log rank test for trend was used. This tested the probability that there was a trend in survival scores across the groups. All tests were two-sided and were determined by Monte Carlo significance. p values <0.05 were considered statistically significant. MedCalc (MedCalc Software, Ostend, Belgium) was used as a complete statistical program. We analyzed Kaplan Meyer curves (Gravina et al., 2017; Colapietro et al., 2020a; Colapietro et al., 2020b) in terms

of hazard ratios (HR), an expression of the ratio of the chance of an event occurring in the treatment arm compared to it occurring in the control arm. For comparisons, HRs were displayed with forest plot graphs.

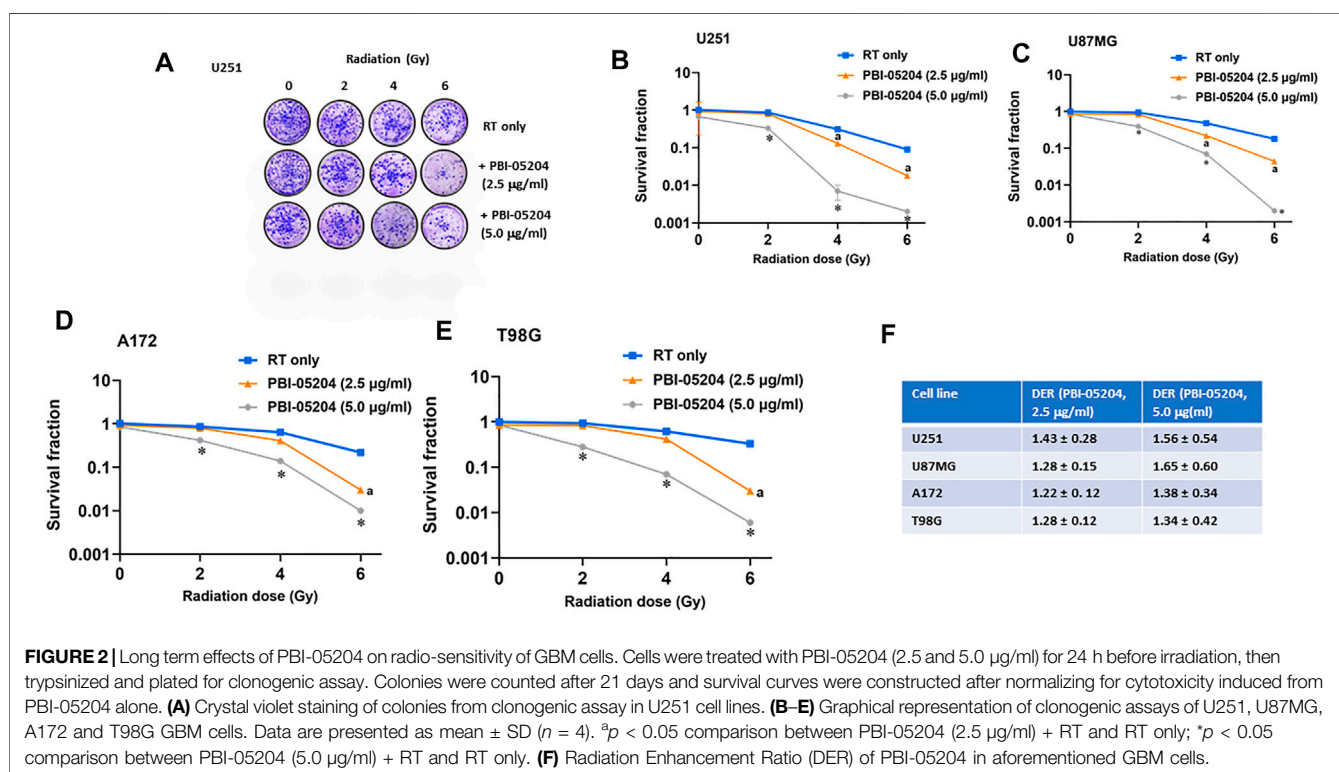
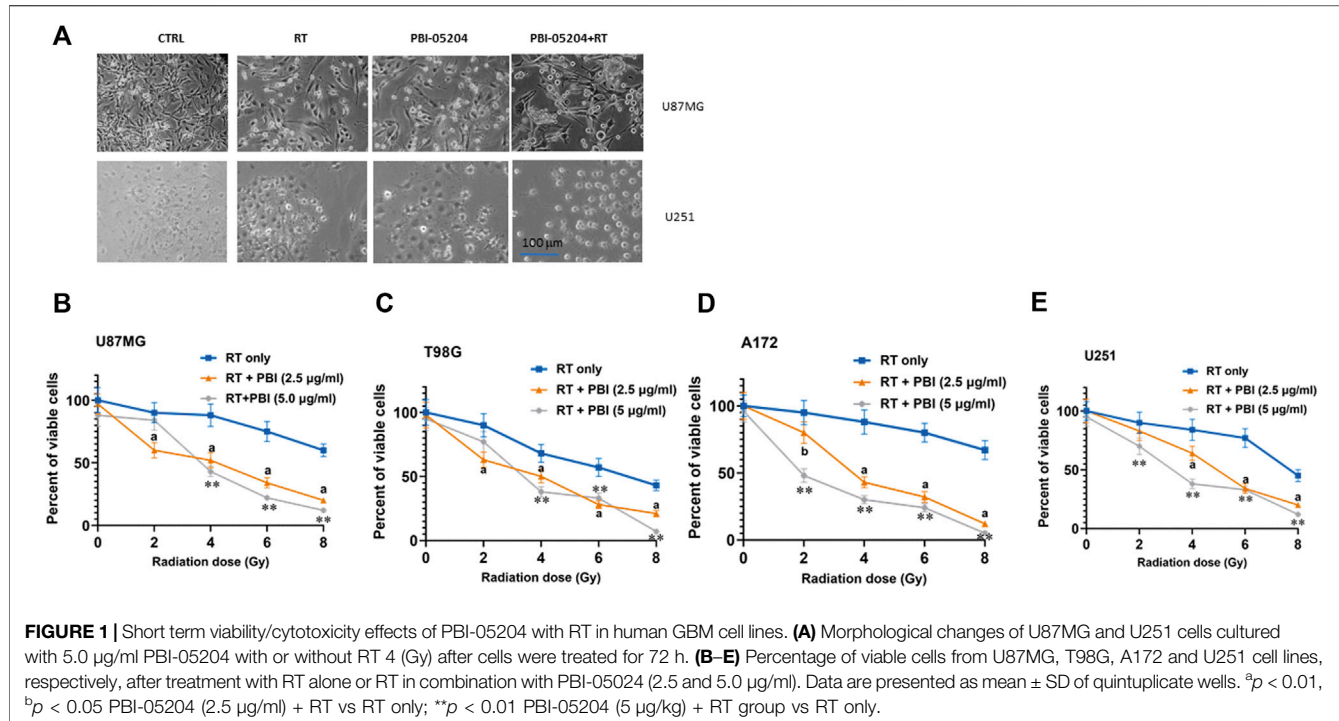
RESULTS

PBI-05204 Exerts Radiosensitizing Effects

We recently demonstrated that PBI-05204 administered to GBM cell lines and patient derived glioma-initiation cells (GICs) showed concentration- and time-dependent anti-proliferative effects (Colapietro et al., 2020a). Morphological, proliferative, and cytotoxic changes were associated with PBI-05204 elicited apoptotic cell death, down-regulation of the PI3K/mTOR pathway and reduction of stemness in GBM cells and GICs. In preparation for studies with radiotherapy, two concentrations of PBI-05204 (2.5 and 5.0 μ g/ml) were chosen for initial *in vitro* studies; these concentrations are close to previously established IC₁₀ and IC₂₀ values in our cell models, respectively. As shown in **Figure 1**, PBI-05204 augmented RT-mediated reduction of cell viability in each of four different established human GBM cell lines. Morphological changes in the appearance of U87MG and U251 (**Figure 1A**) were evident and were accompanied with the concentration-dependent presence of rounded and floating cells. Consistent with this finding, the percent of viable cells determined with a colorimetric assay was notably reduced in PBI-05204 and RT co-treated U87MG (**Figure 1B**), T98G (**Figure 1C**), A172 (**Figure 1D**) and U251 (**Figure 1E**) as opposed to that of RT only group. Concentration dependent changes in percentage of floating, nonviable cells for each cell line are presented in Supplemental data (**Supplementary Figure S1**).

The effect of PBI-05204 on radiation dependent decline in GBM cell clonogenic survival is presented in **Figure 2**. The number and size of colonies stained with crystal violet were reduced when PBI-05204 was co-administered with 2–6 Gy irradiation in U251 cells (**Figure 2A**). Similar changes in clonogenic survival as evidenced by crystal violet staining were noted for U87MG, A172 and T98G colonies as well (data not shown). Quantitation of the dose-dependent radiosensitizing effect of PBI-05204 is evident in the clonogenicity curves of U251, U87MG, A172 and T98G cell lines when they were treated with RT alone (basal treatment) or RT with PBI-05204 (**Figures 2B–E**). Drug Radiotherapy Enhancement (DRE) values were calculated for the cell line survival fractions (**Figure 2F**). The calculated DRE values in all four cell lines ranged between 1.22 and 1.65, suggesting PBI-05204 enhances the anticancer activity of radiation in GBM cells.

The enhanced ability of combining PBI-05204 with RT to control GBM cell proliferation was also evident with examination of established markers of cell proliferation and stemness. As shown in **Supplementary Figure S2**, while PBI-05204 as well as RT independently showed significant reductions in Ki67, CD44 and stro-1 markers in U87MG cells, the combination of PBI-05204 and RT significantly enhanced reduction in expression of all three markers beyond that of either of the two treatment modalities alone.



PBI-05204 Reduces RT-Enhanced Matrigel Invasion and Vasculogenic Mimicry

Studies have suggested that radiation treatment might promote migration and invasion of tumor cells by affecting cell-cell

junctions, induction of epithelial-mesenchymal transition and the tumor microenvironment (Moncharmont et al., 2014). To explore the effects of PBI-05204 on what may be considered an adverse effect of RT on GBM cell migration, the migratory and

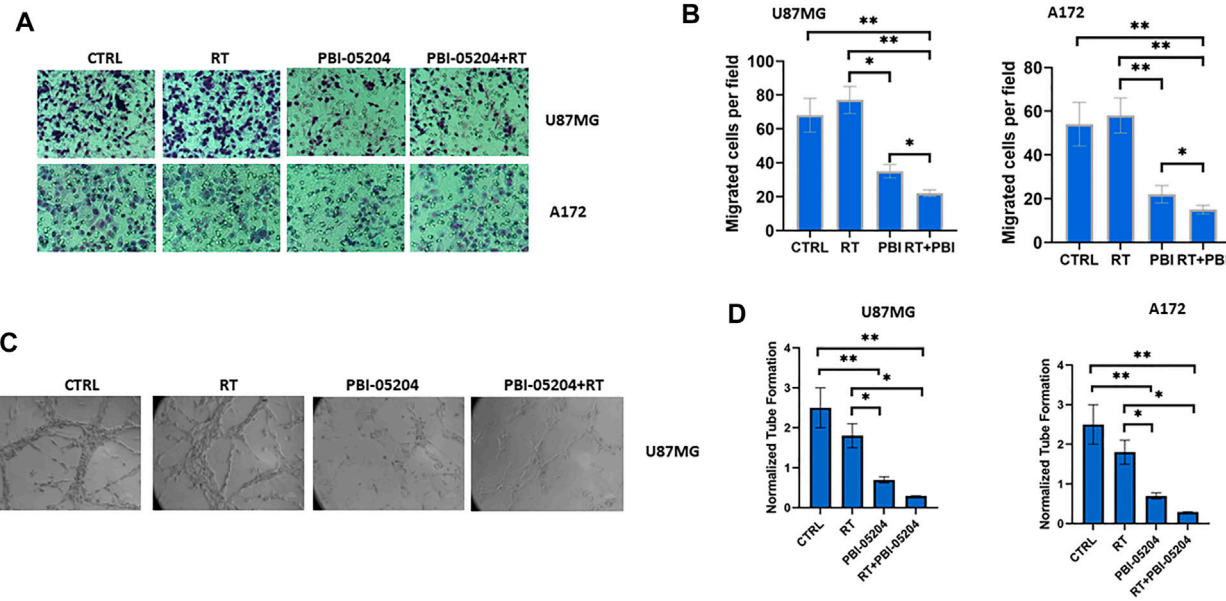


FIGURE 3 | PBI-05204 augmented the antimetastatic and antiangiogenic potential of RT in U87MG and A172 cells. **(A)** Representative images of migrated U87MG and A172 cells. Cell motility through Matrigel-coated filters was measured 6 h after plating. **(B)** Quantitative analyses of the motility of U87MG and A172 cells after treatment with RT (4 Gy), PBI-05204 (5.0 µg/ml) or RT plus PBI-05204. **(C)** Representative images of tubule formation of U87MG cells after treatment with RT, PBI-05204 or RT plus PBI-05204 for 16 h. **(D)** Quantitative analysis of tubule formation in U87 and A172 cells. Data in **(B,D)** are presented as mean ± SD ($n = 4$). * $p < 0.05$ and ** $p < 0.01$.

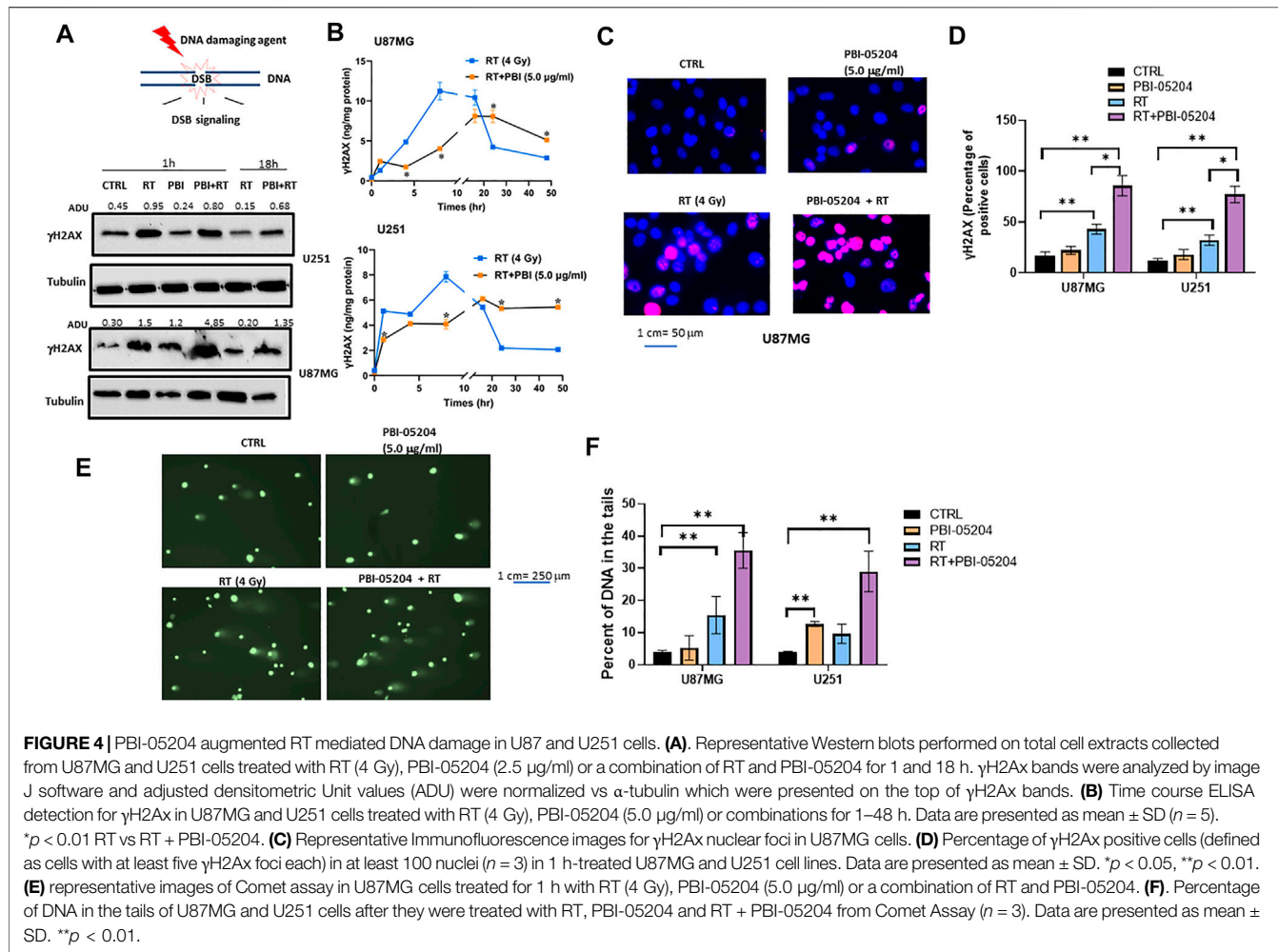
invasive properties of GBM cells were examined. While RT showed a trend of increased invasion and migration of U87MG and A172 cells compared to that of control cells, PBI-05204 alone or in combination with RT led to more than a 50% reduction of both cell migration and invasion compared to vehicle control or RT only treated cells (Figures 3A,B), combination of RT and PBI-05204 showed stronger reduction than PBI-05204 alone. Vasculogenic mimicry is another means of assessing the aggressiveness of GBM cell malignancy. As shown in Figures 3C,D, PBI-05204 alone or in combination with RT significantly reduced tubule formation of U87MG cells and A172 cells by 70 and 90%, respectively, compared to that of vehicle control or RT only groups. Together, these data suggest RT combined with PBI-05204 mitigated RT-mediated cell migration/invasion.

PBI-05204 Enhances Radiosensitivity of GBM by Increasing Double Strand Breaks and Suppressing DNA Damage Repair

In order to explore likely mechanisms wherein PBI-05204 enhances RT mediated cellular effects on GBM cells, the established ability of RT to produce double strand DNA breaks (DSBs) was examined. DSBs were assessed through expression levels of γ-H2AX in GBM cells by Western blot and ELISA assays as well as evaluating both the number of γH2Ax DNA foci for each analyzed nucleus and the number of nuclei affected. U87MG and U251 GBM cells were irradiated at 4 Gy and cultured with or without PBI-05204 (5.0 µg/ml) for

1–48 h. PBI-05204 increased RT-mediated DNA DSBs and was accompanied with an upregulated phosphorylation of Ser 139 of H2Ax (γH2Ax) as shown in Figure 4A. RT was able to increase levels of γH2Ax after only a 1 h treatment in both U251 and U87MG cells. The RT induced higher levels of γH2Ax were reduced after prolonged time of culture indicating a return to baseline over time (Figure 4B). In the analyses performed at 18 h, the levels of γH2Ax in RT treated cells were reduced by more than half of the levels measured at 1 h in both cell lines (Figure 4B). PBI-05204 alone was not particularly able to increase the levels of γH2Ax, but amplified the RT-mediated phosphorylation of this histone as well as slowed down the return to baseline of γH2Ax suggesting a reduction of DNA repair (Figures 4A,B). The increased levels of residual γH2Ax after 18 h of treatment indicates the presence of unrepaired DNA which reflects excessive amount of DNA damage caused by co-administration of RT and PBI-05204, especially at 24 and 48 h of treatment in U87MG and U251 cells (Figure 4B).

The distribution of γH2Ax in U87MG cells treated with RT or RT with PBI-05204 was examined in the U87MG cell line using immunofluorescence staining. The amount of DSBs in RT treated cells was evidenced by enhanced γH2Ax positive staining after 1 h of treatment (Figure 4C). Co-administration of RT with PBI-05204 produced a clearly enhanced phosphorylation of γH2Ax compared to RT alone (Figure 4C) which was in agreement with the Western blot data performed in U87MG cells (Figure 4A) although the level of γH2Ax analyzed by ELISA was either moderately higher or lower in the combination of RT and PBI-05204 than that of RT



alone (Figure 4B). The enhancement of γ H2Ax in U87 and U251 cells after treatment by RT plus PBI-05204 is further demonstrated in Figure 4D where staining indicates DNA damage is more notable for the PBI-05204 + RT treated U87MG and U251 cells compared to that of RT only treated group at 1 h post treatment time. The augmentation of RT induced DNA damage by PBI-05204 in U87MG cells was further supported by the Comet Assay of U87MG cells (Figures 4E,F and Supplementary Table S1).

PBI-05204 Reduced Expression of DNA Repair Enzymes (DNA-PKcs and Rad51)

The effect of PBI-05204 \pm RT on repair of DNA double strand breaks was examined through relative expressions of Ku70, a DNA repair subunit protein, along with DNA-PKcs (DNA-dependent protein kinase catalytic subunit) and RAD51 a protein encoding gene involved with repair of DSBs.

Autophosphorylated DNA-PKcs phosphorylates DSB and binds to heterodimer Ku70/80, which plays a major role in non-homologous end joining (NHEJ) during DNA double strand breaks. On the other hand, RAD51 is a recombinase

protein which promotes homologous pairing and strand exchange during DNA double strand breaks (Jin and Weaver, 1997). Relative increased expression levels of Ku70, DNA-PKcs and RAD51 due to RT were decreased by PBI-05204 (Figures 5A,B). The data in Figure 5A shows that the expression of Ku70 and DNA-PKcs activity (phosphorylated isoform) was particularly reduced at 1 h after PBI-05204 administration in both U87MG and U251 cells, although the effect was not continued at 18 h of treatment (Figure 5A). In contrast, expression of RAD51 protein, a central player in homologous recombination (HR), in U87MG and U251 cells, was down-regulated at both 1 and 18 h after addition of PBI-05204 to RT treatment compared to that of RT only group in which reduced HR efficiency was evidenced by an increased expression of RAD51 protein (Figure 5B). The reduced DNA repair (or the lack of this activity) supported the finding of increased fragmentation of DNA and changes as shown in the comet assay (Figures 4E,F) as well as reduced RAD51 in PBI-05204 and RT co-treated cells compared to that RT only group (Figure 5B). This agrees with the diminished return to baseline of γ H2Ax levels in the time when PBI-05204 was administered in association with RT (as indicated in Figure 4) supporting the

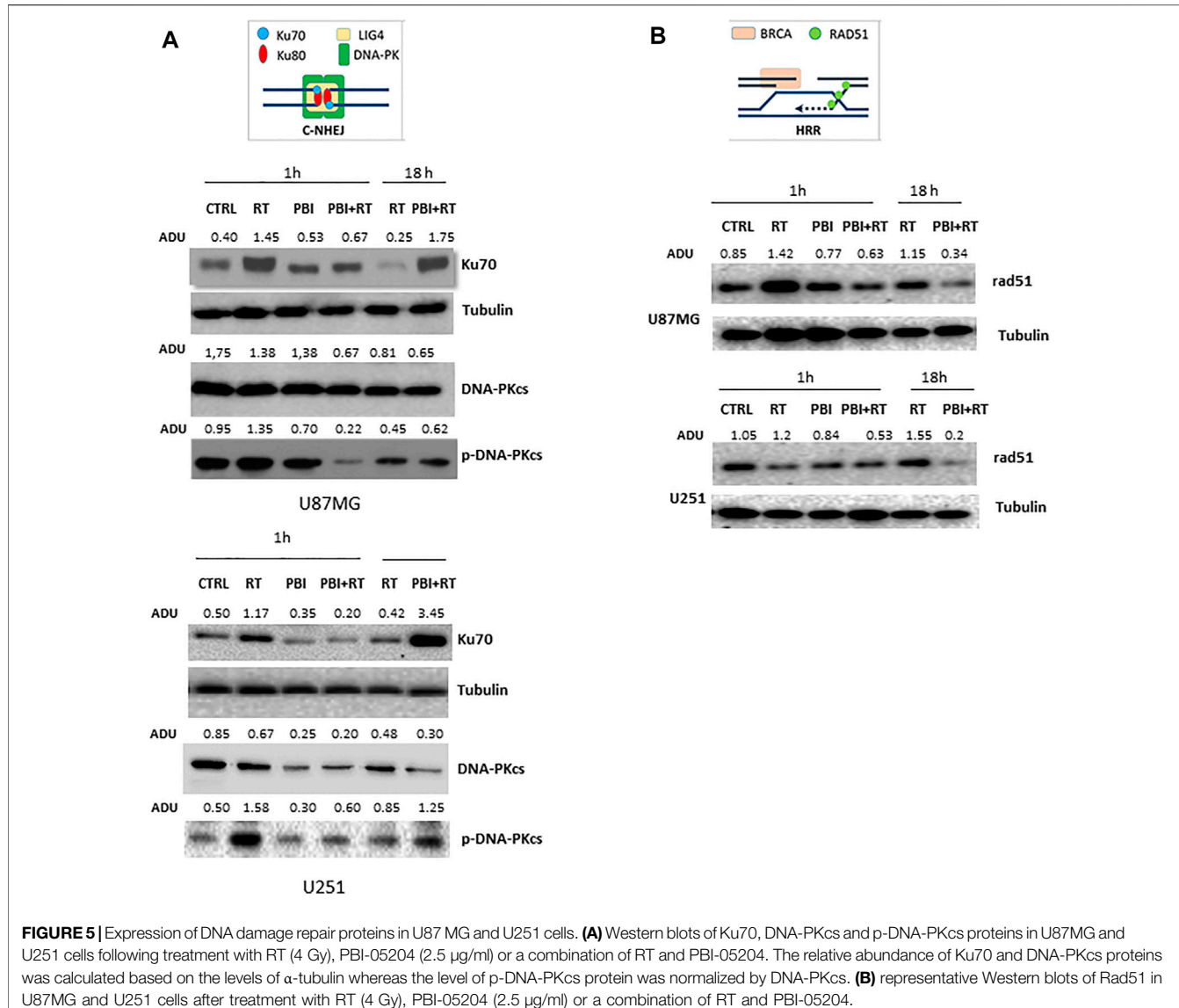


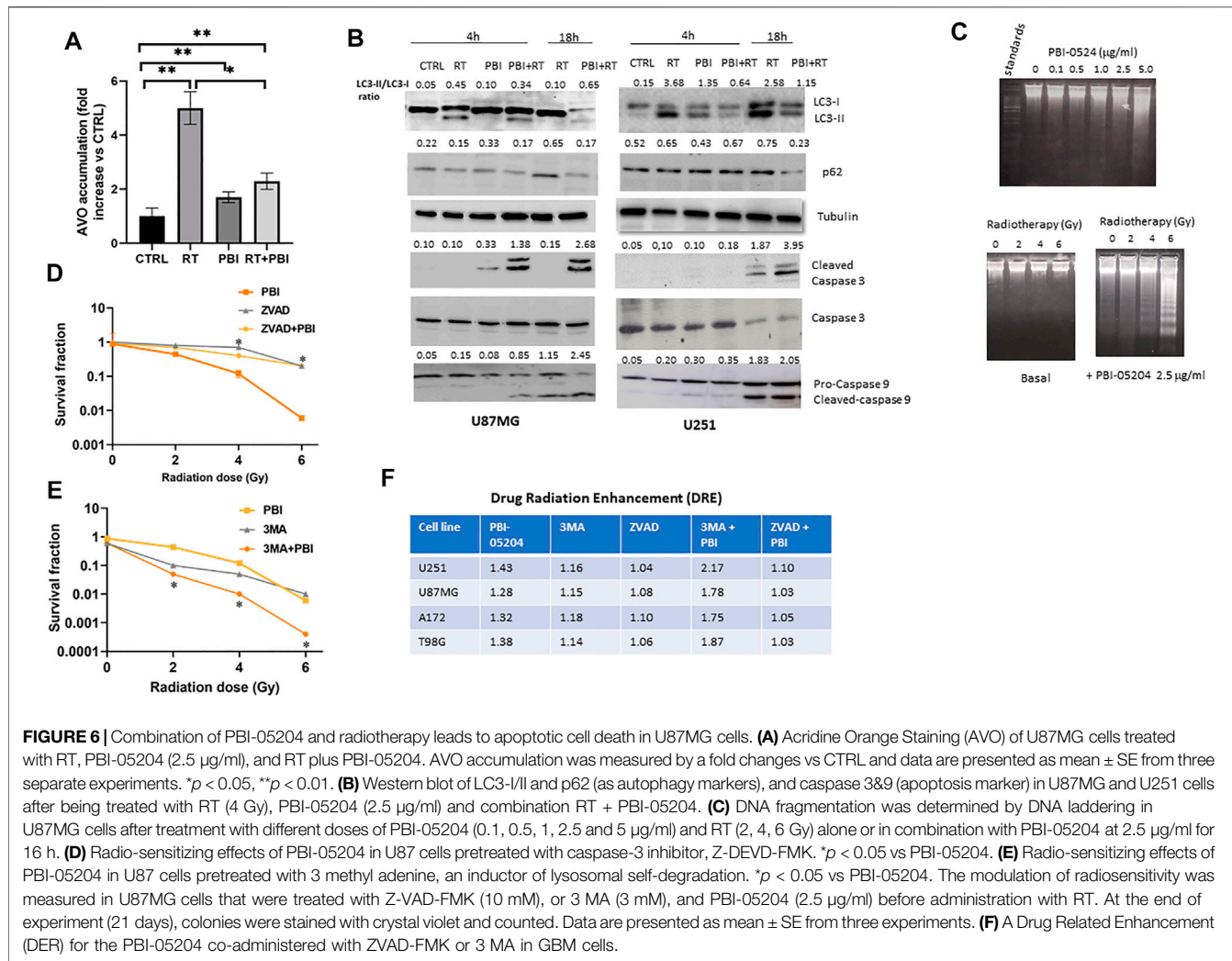
FIGURE 5 | Expression of DNA damage repair proteins in U87 MG and U251 cells. **(A)** Western blots of Ku70, DNA-PKcs and p-DNA-PKcs proteins in U87MG and U251 cells following treatment with RT (4 Gy), PBI-05204 (2.5 µg/ml) or a combination of RT and PBI-05204. The relative abundance of Ku70 and DNA-PKcs proteins was calculated based on the levels of α-tubulin whereas the level of p-DNA-PKcs protein was normalized by DNA-PKcs. **(B)** representative Western blots of Rad51 in U87MG and U251 cells after treatment with RT (4 Gy), PBI-05204 (2.5 µg/ml) or a combination of RT and PBI-05204.

hypothesis that administration of PBI-05204 reduced RT-mediated DNA repair resulting in increased sensitivity to RT.

PBI-05204 Increased RT Mediated Cell Death by Induction of Caspase Activity (Apoptosis) and Reduced Induction of Autophagy

The effects of RT (4 Gy) and PBI-05204 (5 µg/ml) on the morphology of nuclei indicative of autophagy and apoptotic changes were examined by using Acridine Orange (AO) and Hoechst 3324 staining. As shown in **Supplementary Figures S3A,B**, RT treated cells exhibited a concentration dependent enhancement in staining with acridine orange, a dye for detection of acidic vesicular organelles (AVOs), suggesting RT treated cells were undergoing induction of autophagy. While only

a moderate alteration on acridine orange staining in U251 cells treated with PBI-05204 alone (**Supplementary Figures S3A,B**) was evident, a substantial decrease in AVO staining occurred when PBI-05204 was combined with RT treatment (**Figure 6A**) suggesting that PBI-05204 lessened the level of autophagy induced by RT in U87MG cells. In contrast, clear changes in nuclear morphology were observed starting from 24 h of co-administration of PBI-05204 and RT (**Supplementary Figure S3C**) indicating an induction of early apoptotic events. Consistently, the ratio of the well known autophagy marker LC3-II/LC3-I was highly elevated in RT treated U251 cells compared to that of the control group at both 1 and 18 h treatment, whereas addition of PBI-05204 to RT treated cells led to a reduced ratio of the LC3-II/LC3-I in comparison with that of RT only treated cells (**Figure 6B**) which is consistent with the observed extent of acridine orange staining. Furthermore, the



levels of both cleaved caspase 3 and 9, representative makers for apoptotic cell death, were higher in combination of RT and PBI-05204 treated cells than that of RT alone treated cells (**Figure 6B**). PBI-05204 alone or in combination with RT treated cells showed increased DNA fragmentation in a concentration-dependent manner in U87MG compared to that of vehicle control whereas RT only treated cells failed to induce DNA fragmentation (**Figure 6C**). Similarly, caspase 3 and caspase 9 were activated (**Supplementary Figure S3D**) in the GBM cells treated with PBI-05204 and RT and the subG1 phase of U87MG cell population was four-fold higher following treatment with of PBI-05204 and RT compared to that of the RT only group (**Supplementary Figure S3E**). Furthermore, inhibition of caspase-3 activation with Z-DEVD-FMK (**Figure 6D**) abrogated the PBI-05204-induced enhancement of radiation response whereas the addition of 3 methyl adenine, an inductor of lysosomal self-degradation, instead, increased the effects of PBI-05204 to RT (**Figure 6E**). This is further supported by the value of DER in the U87MG, A172, U21 and T98G (**Figure 6F**) indicating that autophagy may be an inhibitor of radio-sensitivity and PBI-05204 reduced

radiotherapy induced autophagic cell death and enhanced apoptosis in GBM cells.

PBI-05204 Enhances Radiosensitivity In Vivo

The antitumor effects of PBI-05204 alone and in combination with RT were evaluated *in vivo* in U251, U87MG, and T98G GBM xenograft models. In **Figure 7A**, the treatment plan of RT, PBI-05204, and RT plus PBI-05204 in mice bearing GBM xenografts is shown. In the U87MG model, the combination PBI-05204 plus RT significantly reduced tumor weight by 78% ($p < 0.0001$) while single treatment of either modality showed reductions of 56% (PBI-05204, $p < 0.0001$) and 14% (RT) compared to that of vehicle control group (**Figures 7B,C**). PBI-05204 significantly enhanced the RT mediated inhibition of tumor growth by almost six-fold in this model evidenced by both tumor volume and terminal tumor weights (**Figure 7C**). Similarly, the average U251 terminal tumor weights of mice treated with PBI-05204 and RT was 375 ± 66 mg which was significantly smaller than that of vehicle control (918 ± 240 mg) or RT only groups (677 ± 132 mg),

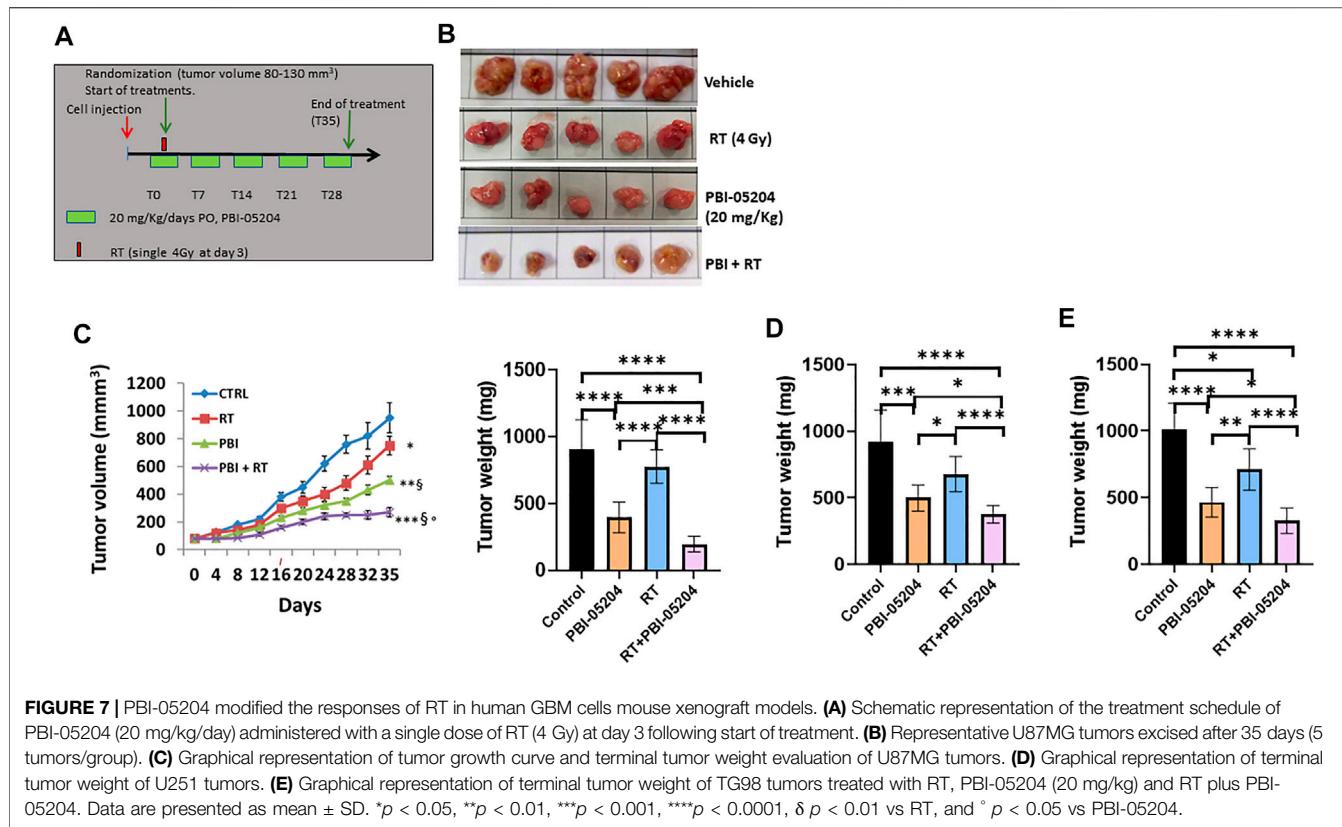


FIGURE 7 | PBI-05204 modified the responses of RT in human GBM cells mouse xenograft models. **(A)** Schematic representation of the treatment schedule of PBI-05204 (20 mg/kg/day) administered with a single dose of RT (4 Gy) at day 3 following start of treatment. **(B)** Representative U87MG tumors excised after 35 days (5 tumors/group). **(C)** Graphical representation of tumor growth curve and terminal tumor weight evaluation of U87MG tumors. **(D)** Graphical representation of terminal tumor weight of U251 tumors. **(E)** Graphical representation of terminal tumor weight of TG98 tumors treated with RT, PBI-05204 (20 mg/kg) and RT plus PBI-05204. Data are presented as mean \pm SD. * p < 0.05, ** p < 0.01, *** p < 0.001, **** p < 0.0001, δ p < 0.01 vs RT, and \circ p < 0.05 vs PBI-05204.

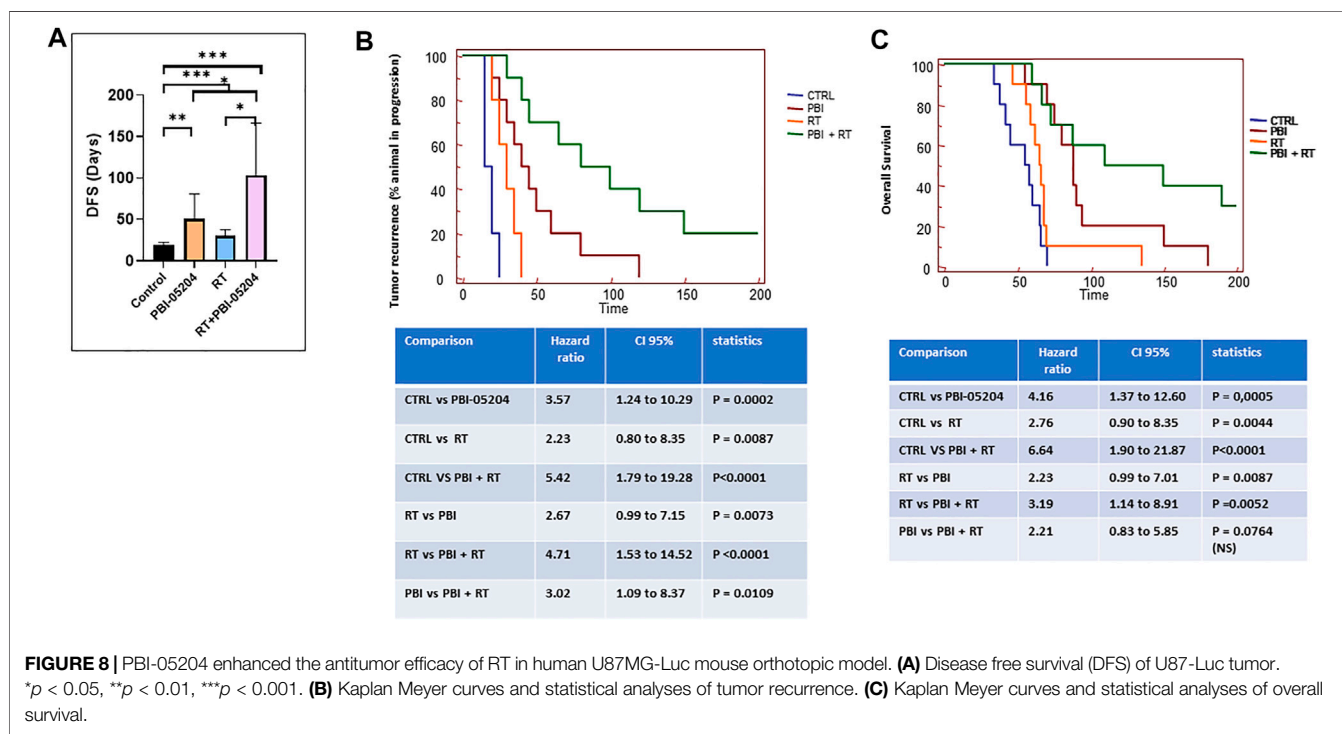


FIGURE 8 | PBI-05204 enhanced the antitumor efficacy of RT in human U87MG-Luc mouse orthotopic model. **(A)** Disease free survival (DFS) of U87-Luc tumor. * p < 0.05, ** p < 0.01, *** p < 0.001. **(B)** Kaplan Meyer curves and statistical analyses of tumor recurrence. **(C)** Kaplan Meyer curves and statistical analyses of overall survival.

respectively (p < 0.0001) (Figure 7D). Tumor weight data derived from mice bearing TG98 xenografts showed a similar enhanced response to PBI-05204 plus radiotherapy compared to either

individual treatment modality (Figure 7E). The growth curve of both U251 and T98G mouse xenografts also further supports the radiosensitizing effect of PBI-05204 (Supplementary Figure S4).

PBI-05204 Inhibits Intracranial Tumor Growth and Augments RT Antitumor Efficacy

The antitumor efficacy of PBI-05204 in combination with RT was further investigated in orthotopically implanted U87-Luciferase labeled tumors. Disease-Free Survival (DFS) values were calculated for vehicle (CTRL), PBI-05204 (20 mg/kg/day), RT (4Gy) and PBI-05204 plus RT treatments (**Figure 8**). Control mice developed bioluminescent detectable lesions between 10 and 35 days after tumor implantation with a mean of 18.5 ± 4.1 days. RT (4 Gy) was able to increase the DFS and slowed tumor recurrence up 30 days. PBI-05204 significantly increased DFS up to 50.5 ± 30.1 days compared to control animals ($p < 0.0037$) (**Figure 8A**). The combination of RT and PBI-05204 showed a significant enhancement of DFS to 103.0 ± 63.2 days compared to the control group ($p = 0.0005$) which was three-fold longer than that of the RT only group (**Figure 8A**). Intriguingly, there were 20% RT plus PBI-05204 treated mice with undetectable tumors at 200 days post tumor implantation (**Figure 8B**). The combination of RT and PBI-05204 resulted in a significant enhancement of overall survival compared to either single treatment modality alone (**Figure 8C**). For example, the average overall survival of mice treated with PBI-05204 plus RT was 138.8 ± 60.4 days which was significantly longer than control mice (53.4 ± 12.7 days, $p = 0.0008$) and RT treated mice (71.0 ± 11.6 days, $p = 0.0027$), suggesting PBI-05204 is capable of enhancing the antitumor efficacy of radiotherapy in GBM.

DISCUSSION

The overall purpose of the present study was to evaluate the effect of PBI-05204 on radiosensitivity in GBM. We previously demonstrated PBI-05204 showed a dose-dependent effectiveness in both *in vitro* and *in vivo* GBM models (Colapietro et al., 2020a). Here we found that addition of PBI-05204 to RT significantly enhanced the anti-proliferative and antitumor activity of RT in both *in vitro* GBM cells and *in vivo* human GBM cells mouse xenograft or orthotopic tumors. The radiosensitization of PBI-05204 appears to be mediated by a reduction of autophagy and promotion of apoptosis as well as reduced DNA repair. Although we previously reported radiosensitization due to use of oleandrin, an active component of PBI-05204, in prostate cancer PC3 cells (Nasu et al., 2002), this is the first study demonstrating the radiosensitization potential of PBI-05204 in GBM cells and relevant tumor tissues. Given that resistance to chemotherapy and radiation is a major challenge for the successful treatment of GBM and that PBI-05204 has already been tested in both phase I and phase II clinical trials for solid tumors, our findings suggest that PBI-05204 could be a potentially efficacious adjuvant treatment of radiation for patients with GBM.

DNA damage is one of the major targets of radiation in the cellular system, and the DNA repair pathway is one of the main causes of resistance to radiation (Huang and Zhou, 2020). RT-induced cell death occurs due to DNA damage, leading to DNA

double-strand breaks (DSBs). Subsequently, tumor cells with highly efficient DNA repair mechanisms tend to be radioresistant whereas deficiencies in pathways that repair DSBs are especially unfavorable to the cells. Error prone non homologous endjoining (NHEJ) or error free homologous recombination are major pathways being targeted during cancer therapy (Shrivastav et al., 2008). Radiotherapy in combination with surgery and chemotherapy in GBM is a preferred treatment regime although GBM is usually resistant to any such conventional treatment process due to tumor heterogeneity. It has been previously reported that inhibition of RAD51 prevents IR induced DNA repair and is linked to poor prognosis in GBM patients (King et al., 2017). Similarly, DNA-PKcs is crucial for maintenance of glioblastoma stem cells and is a potential therapeutic target for the treatment of glioblastoma (Fang et al., 2021). Changes in the levels of DNA repair proteins have been correlated with resistance to anti-cancer strategies (Miyashita et al., 2021). The DNA damage response (DDR) pathway is known to play an important role in both radioresistance and radiosensitization (Raleigh and Haas-Kogan, 2013). DNA damage is initially identified by sensor proteins, including the Mre11-rad50-nbs (MRN) complex, ATRIP and Ku70/80 which results in rapid activation of the signal transduction kinases, such as ATM, ATR and DNA-PKcs. Atypical activation of DNA damage checkpoints and enhanced DNA repair in glioblastoma stem cells causes radioresistance of GBM tumors (Bao et al., 2006), whereas reduction or loss of DDR components can sensitize cells to the cytotoxic effect of radiation. In line with this, we and others have reported that inhibition of the DNA-dependent protein kinase catalytic subunit radiosensitizes GBM and GSCs by inducing apoptotic cell death (Timme et al., 2018; Fang et al., 2021). Many studies have also shown that natural compounds can inhibit DNA repair machinery when coupled with radiation, thereby acting as radio-sensitizing agents (Peterson, 2019). In our study, we observed that PBI-05204 could attenuate DNA repair after RT as indicated by increased expression and permanence of γ H2AX over time and reduction of Rad51 and DNA-PKcs. Inhibition of both PI3Kinase and mTOR pathways can potently downregulate two central DDR kinase, DNA-PKcs and ATM as well as RAD51 resulting in radiosensitization in GBM and GSC cells (Wang et al., 2013; Djuzenova et al., 2021). Given that PBI-05204 is capable of down regulating PI3K and mTOR pathways in both pancreatic cancer and GBM (Pan et al., 2015), whether PBI-05204 elicited reduction of DNA repair caused by RT is mediated through reduction of PI3K/mTOR pathway by PBI-05204 is deserving of further investigation.

It has been reported that oleandrin can inhibit the proliferation of various tumor cells and enhance antiproliferative potential of radiation to prostate cancer cells by induction of apoptosis (Nasu et al., 2002; Kanwal et al., 2020). Treatment with PBI-05204 has also been reported to lead to apoptotic cell death by activation of caspases 3, 8 and 9 and down-regulation of PI3kinase/mTOR pathways evidenced by reduced expression of pAKT, pS6 and p4EBP1 in GBM cells (Colapietro et al., 2020a). As autophagy is a well-known factor contributing to radioresistance (Chen et al., 2017) and induction of apoptotic cell

death has been one of the key mechanisms responsible for radiosensitization, we investigated whether PBI-05204 sensitizing radiotherapy treatment is mediated by a reduction of autophagic cell death and increased apoptosis in GBM cells. We found that U251 cells treated with RT alone substantially increased staining with Acridine Orange indicative of autophagic cell death whereas the combination of PBI-05204 and RT leads to an almost 50% reduction of AO staining compared to that of RT alone. In contrast, while treatment with RT alone did not induce any measurable amount of activated caspase-3 and moderate apoptotic cell death, pretreatment of GBM cells with PBI-05204 significantly increased sensitivity to apoptosis induction by RT. This is associated with mitochondrial damage (mitochondria pathways of apoptosis) and associated caspase 9 activation and with death receptor mediated cell death with caspase 8 activation. The important role of apoptosis in PBI-05204 elicited radiosensitization in GBM cells is further supported by the evidence that a caspase-3 inhibitor abolished PBI-induced enhancement of radiosensitivity. Whether the induction of apoptotic cell death in PBI-05204 and RT treated GBM cells is primarily due to the bioactive component of oleandrin is strongly suggested from prior studies but remains to be determined as a principal pharmacologic agent supporting enhancement of radiotherapy.

GSCs have been found to contribute to the recurrence and resistance to irradiation, a major therapeutic modality for the treatment of unresectable glioblastomas (Barani and Larson, 2015). Emerging evidence suggests that cancer stem cells (CSCs) are capable of self-renewal and are refractory to cancer treatment. Thus, cancer stem cells including GSCs have become a primary target for anti-cancer therapy. Previously our study showed that PBI-05204 can reduce the stemness and downregulate stemness markers in GBM cells (Colapietro et al., 2020a). Here we also demonstrated that the combination of PBI-05204 and RT significantly reduced the colony formation capacity of GSCs as evidenced by a reduction in the amount and size of the newly formed neurospheres and the level of neural stem cell markers including SOX2, Oct3/4, CD44 and Stro-1 in PBI-05204 and RT co-treated GBM cells, which was consistent with previously published reports (Colapietro et al., 2020a). The synergistic effect of PBI-05204 and RT in increasing radio-sensitization of GSCs was also demonstrated in the animal models *in vivo*. Combined treatment with PBI-05204 and RT resulted in a substantial growth delay and subsequent inhibition of the growth rate of tumor in the mice bearing U87MG GSCs. These results strongly suggest that combined treatment with PBI-05204 and RT deregulated the self-renewal of GSCs and reduced the stemness of GSCs. DNA damage repair capacity following RT, especially regarding DNA double strand breaks (DSB), has been shown to be higher in CSC, including GSCs, compared to their non-tumorigenic counterparts. Considering that addition of PBI-05204 to RT treated cells slows the DNA repair process in GBM cells, further research needs to be conducted to understand whether the reduced DNA repair capacity of PBI-05204 is associated with its effect on GSCs. Such studies are currently underway.

This present study has some limitations. The first limitation involves an adequate understanding of the influence of RT alone and RT plus PBI-05204 on expression of γ H2Ax of GBM cells. As our data suggest that PBI-05204 appears to enhance the radiotherapeutic efficacy in GBM cells and DNA damage is one of the major mechanisms associated with radiosensitivity, we set out to test whether the radiosensitizing effect of PBI-05204 is mediated by the enhanced DNA damage that is caused by RT alone by examining the level of γ H2Ax and by use of Comet assays. The western blot analysis (Figure 4A), ELISA analysis (Figure 4B) and immunofluorescence images for γ H2Ax nuclear foci (Figures 4C,D) in U87MG and U251 cells demonstrate that the accumulation γ H2AX was more pronounced after 18 h of treatment with PBI-05204 and RT whereas the γ H2AX in RT alone treated cells peaked around 8 h. In fact, the levels of γ H2AX in RT alone treated cells decreased after 8 h suggesting DNA repair events may occur after this time. A more complete understanding of how addition of PBI-05204 to RT treatment influences DNA damage caused by RT between 1 and 8 h of treatment requires further investigation with respect to the exhibited discrepancy on accumulation of γ H2AX assessed by western blot and ELISA assays in aforementioned GBM cells. Our data demonstrates the accumulation of γ H2Ax in PBI-05204 and RT treated U87MG cells. These levels remained elevated until 24 h after treatment in U87MG and 48 h in U251 cells. The data derived from Comet Assays also suggests that PBI-05204 addition to RT treatment leads to a notably higher percentage of DNA in the Commet tails than that of RT alone. The data overall suggest thats PBI-05204 treatment leads to enhanced DNA damage caused by RT.

A second limitation may lie in interpretation of the DNA repair mechanism responsible for radiosensitization of PBI-05204 in GBM cells. While the rH2Ax data suggests a slower DNA repair process with addition of PBI-05204, we explored the role of two important DSB repair mechanisms, NHEJ and HR, on inhibition of DNA repair caused by PBI-05204 in GBM cells. The data suggest that the slower repair of DSB in cells treated with PBI-05204 and RT might principally be due to the HR repair mechanism due to the fact that both Ku70 and pDNA-Pkc levels were higher in RT + PBI-05204 than that of RT alone at 18 h even though they were lower after 1 h treatment (Figure 5A). In contrast, RAD51 expression remained low at both 1 and 18 h after the treatment of RT and PBI-05204 compared to that of the RT only group. Although the HR mechanism is only a portion of the overall DSB repair pathway compared to NHEJ, studies suggest that RAD51 is very important for radiosensitivity of GSCs and GSCs appear to prefer using the HR instead of NHEJ repair mechanism for DSB (Balbous et al., 2016). Additionally, a recent study has shown that overexpression of RAD51 is associated with poor prognosis in patients with GBM suggesting the importance of RAD51 in GBM (Morrison et al., 2021). While the slower repair process of DSB in RT and PBI-05204 treated GBM cells could be mediated by the committant impairment of NHEJ and HR, our data suggest that the HR repair mechanism might play a major role in PBI-05204 elicited slower DNA repair process caused by RT. Additional research is needed to further confirm

how PBI-05204 affects the repair of DNA damage caused by RT.

In conclusion, our data demonstrate that co-administration of PBI-05204 and RT can be a potential advantageous therapeutic strategy for treating GBM. The radio-sensitization effect of PBI-05204 was supported by impaired capacity for DNA repair in the early stage, inhibition of proliferation and stemness, and promotion of apoptosis *in vitro* and *in vivo*. Collectively, these results demonstrate that PBI-05204 is a potential radiation sensitizer for malignant glioma treatment and warrants further investigation.

DATA AVAILABILITY STATEMENT

The original contributions presented in the study are included in the article/**Supplementary Material**, further inquiries can be directed to the corresponding authors.

ETHICS STATEMENT

The animal study was reviewed and approved by University of L'Aquila, Medical School and Science and Technology School Board Regulations, complying with the Italian government regulation n.116 January 27, 1992 for the use of laboratory animals.

REFERENCES

- Auffinger, B., Spencer, D., Pytel, P., Ahmed, A. U., and Lesniak, M. S. (2015). The Role of Glioma Stem Cells in Chemotherapy Resistance and Glioblastoma Multiforme Recurrence. *Expert Rev. Neurother* 15 (7), 741–752. doi:10.1586/14737175.2015.1051968
- Balbous, A., Cortes, U., Guilloteau, K., Rivet, P., Pinel, B., Duchesne, M., et al. (2016). A Radiosensitizing Effect of RAD51 Inhibition in Glioblastoma Stem-Like Cells. *BMC Cancer* 16, 604. doi:10.1186/s12885-016-2647-9
- Bao, S., Wu, Q., McLendon, R. E., Hao, Y., Shi, Q., Hjelmeland, A. B., et al. (2006). Glioma Stem Cells Promote Radioresistance by Preferential Activation of the DNA Damage Response. *Nature* 444 (7120), 756–760. doi:10.1038/nature05236
- Barani, I. J., and Larson, D. A. (2015). Radiation Therapy of Glioblastoma. *Cancer Treat. Res.* 163, 49–73. doi:10.1007/978-3-319-12048-5_4
- Chen, X., Wang, P., Guo, F., Wang, X., Wang, J., Xu, J., et al. (2017). Autophagy Enhanced the Radioresistance of Non-Small Cell Lung Cancer by Regulating ROS Level under Hypoxia Condition. *Int. J. Radiat. Biol.* 93 (8), 764–770. doi:10.1080/09553002.2017.1325025
- Colapietro, A., Mancini, A., Vitale, F., Martellucci, S., Angelucci, A., Llorens, S., et al. (2020). Crocetin Extracted from Saffron Shows Antitumor Effects in Models of Human Glioblastoma. *Int. J. Mol. Sci.* 21 (2), 423. doi:10.3390/ijms21020423
- Colapietro, A., Yang, P., Rossetti, A., Mancini, A., Vitale, F., Martellucci, S., et al. (2020). The Botanical Drug PBI-05204, a Supercritical CO₂ Extract of Nerium Oleander, Inhibits Growth of Human Glioblastoma, Reduces Akt/mTOR Activities, and Modulates GSC Cell-Renewal Properties. *Front. Pharmacol.* 11, 552428. doi:10.3389/fphar.2020.552428
- Djuzenova, C. S., Fischer, T., Katzer, A., Sisario, D., Korsa, T., Steussloff, G., et al. (2021). Opposite Effects of the Triple Target (DNA-PK/PI3K/mTOR) Inhibitor PI-103 on the Radiation Sensitivity of Glioblastoma Cell Lines Proficient and Deficient in DNA-PKcs. *BMC Cancer* 21 (1), 1201. doi:10.1186/s12885-021-08930-1
- Fang, X., Huang, Z., Zhai, K., Huang, Q., Tao, W., Kim, L., et al. (2021). Inhibiting DNA-PK Induces Glioma Stem Cell Differentiation and Sensitizes Glioblastoma to Radiation in Mice. *Sci. Transl. Med.* 13 (600), eabc7275. doi:10.1126/scitranslmed.abc7275
- Granzotto, A., Joubert, A., Vieu, M., Devic, C., Maalouf, M., Thomas, C., et al. (2011). Individual Response to Ionizing Radiation: What Predictive Assay(s) to Choose? *C R. Biol.* 334 (2), 140–157. doi:10.1016/j.crvi.2010.12.018
- Gravina, G. L., Mancini, A., Mattei, C., Vitale, F., Marampon, F., Colapietro, A., et al. (2017). Enhancement of Radiosensitivity by the Novel Anticancer Quinolone Derivative Vosaroxin in Preclinical Glioblastoma Models. *Oncotarget* 8 (18), 29865–29886. doi:10.18632/oncotarget.16168
- Gravina, G. L., Mancini, A., Scarsella, L., Colapietro, A., Jitariuc, A., Vitale, F., et al. (2016). Dual PI3K/mTOR Inhibitor, XL765 (SAR245409), Shows Superior Effects to Sole PI3K [XL147 (SAR245408)] or mTOR [rapamycin] Inhibition in Prostate Cancer Cell Models. *Tumour Biol.* 37 (1), 341–351. doi:10.1007/s13277-015-3725-3
- Gravina, G. L., Marampon, F., Sherris, D., Vittorini, F., Di Cesare, E., Tombolini, V., et al. (2014). Torc1/Torc2 Inhibitor, Palomid 529, Enhances Radiation Response Modulating CRM1-Mediated Survivin Function and Delaying DNA Repair in Prostate Cancer Models. *Prostate* 74 (8), 852–868. doi:10.1002/pros.22804
- Haque, A., Banik, N. L., and Ray, S. K. (2011). Molecular Alterations in Glioblastoma: Potential Targets for Immunotherapy. *Prog. Mol. Biol. Transl. Sci.* 98, 187–234. doi:10.1016/B978-0-12-385506-0-00005-3
- Hong, D. S., Henary, H., Falchook, G. S., Naing, A., Fu, S., Moulder, S., et al. (2014). First-in-human Study of Pbi-05204, an Oleander-Derived Inhibitor of Akt, Fgf-2, Nf-κB and P70s6k, in Patients with Advanced Solid Tumors. *Invest. New Drugs* 32 (6), 1204–1212. doi:10.1007/s10637-014-0127-0
- Huang, R. X., and Zhou, P. K. (2020). DNA Damage Response Signaling Pathways and Targets for Radiotherapy Sensitization in Cancer. *Signal. Transduct. Target. Ther.* 5 (1), 60. doi:10.1038/s41392-020-0150-x
- Jin, S., and Weaver, D. T. (1997). Double-Strand Break Repair by Ku70 Requires Heterodimerization with Ku80 and DNA Binding Functions. *EMBO J.* 16 (22), 6874–6885. doi:10.1093/emboj/16.22.6874
- Kanwal, N., Rasul, A., Hussain, G., Anwar, H., Shah, M. A., Sarfraz, I., et al. (2020). Oleandrin: A Bioactive Phytochemical and Potential Cancer Killer via Multiple Cellular Signaling Pathways. *Food Chem. Toxicol.* 143, 111570. doi:10.1016/j.fct.2020.111570

AUTHOR CONTRIBUTIONS

CF, PY, FM, VM, GG, and RN designed and supervised research. AC, AR, AM, FV, and SM performed the experiments. PY, GG, and CF analyzed data. PY, SC, RN, RI, and CF wrote or reviewed the manuscript. All authors contributed to the article and approved the submitted version.

FUNDING

The authors declare that this study was partially supported by a research grant from Phoenix Biotechnology, Inc. (San Antonio, TX, United States). The funder was not involved in the study design, collection, analysis, interpretation of data, the writing of this article or the decision to submit it for publication. This work was also partially supported by a research grant from the ALCLI “Giorgio e Silvia” a Non-Profit Association.

SUPPLEMENTARY MATERIAL

The Supplementary Material for this article can be found online at: <https://www.frontiersin.org/articles/10.3389/fphar.2022.852941/full#supplementary-material>

- King, H. O., Brend, T., Payne, H. L., Wright, A., Ward, T. A., Patel, K., et al. (2017). RAD51 Is a Selective DNA Repair Target to Radiosensitize Glioma Stem Cells. *Stem Cel Rep.* 8 (1), 125–139. doi:10.1016/j.stemcr.2016.12.005
- Lathia, J. D., Mack, S. C., Mulkearns-Hubert, E. E., Valentim, C. L., and Rich, J. N. (2015). Cancer Stem Cells in Glioblastoma. *Genes Dev.* 29 (12), 1203–1217. doi:10.1101/gad.261982.115
- Lawrence, T. S. (1988). Ouabain Sensitizes Tumor Cells but Not Normal Cells to Radiation. *Int. J. Radiat. Oncol. Biol. Phys.* 15 (4), 953–958. doi:10.1016/0360-3016(88)90132-0
- Li, X., Zheng, J., Chen, S., Meng, F. D., Ning, J., and Sun, S. L. (2021). Oleandrin, a Cardiac Glycoside, Induces Immunogenic Cell Death via the PERK/eIF2α/ATF4/CHOP Pathway in Breast Cancer. *Cell Death Dis* 12 (4), 314. doi:10.1038/s41419-021-03605-y
- Lin, Y., Dubinsky, W. P., Ho, D. H., Felix, E., and Newman, R. A. (2008). Determinants of Human and Mouse Melanoma Cell Sensitivities to Oleandrin. *J. Exp. Ther. Oncol.* 7 (3), 195–205.
- Liu, Y. C., Yeh, C. T., and Lin, K. H. (2020). Cancer Stem Cell Functions in Hepatocellular Carcinoma and Comprehensive Therapeutic Strategies. *Cells* 9 (6), 1331. doi:10.3390/cells9061331
- Mattei, V., Santilli, F., Martellucci, S., Delle Monache, S., Fabrizi, J., Colapietro, A., et al. (2021). The Importance of Tumor Stem Cells in Glioblastoma Resistance to Therapy. *Int. J. Mol. Sci.* 22 (8), 3863. doi:10.3390/ijms22083863
- Miyashita, S., Owa, T., Seto, Y., Yamashita, M., Aida, S., Sone, M., et al. (2021). Cyclin D1 Controls Development of Cerebellar Granule Cell Progenitors through Phosphorylation and Stabilization of ATOH1. *EMBO J.* 40 (14), e105712. doi:10.1525/embj.2020105712
- Moncharmont, C., Levy, A., Guy, J. B., Falk, A. T., Guilbert, M., Trone, J. C., et al. (2014). Radiation-Enhanced Cell Migration/invasion Process: A Review. *Crit. Rev. Oncol. Hematol.* 92 (2), 133–142. doi:10.1016/j.critrevonc.2014.05.006
- Morrison, C., Weterings, E., Mahadevan, D., Sanan, A., Weinand, M., and Stea, B. (2021). Expression Levels of RAD51 Inversely Correlate with Survival of Glioblastoma Patients. *Cancers (Basel)* 13 (21), 5358. doi:10.3390/cancers13215358
- Nasu, S., Milas, L., Kawabe, S., Raju, U., and Newman, R. (2002). Enhancement of Radiotherapy by Oleandrin Is a Caspase-3 Dependent Process. *Cancer Lett.* 185 (2), 145–151. doi:10.1016/s0304-3835(02)00263-x
- Pan, Y., Rhea, P., Tan, L., Cartwright, C., Lee, H. J., Ravoori, M. K., et al. (2015). PBI-05204, a Supercritical CO₂ Extract of Nerium Oleander, Inhibits Growth of Human Pancreatic Cancer via Targeting the PI3K/mTOR Pathway. *Invest. New Drugs* 33 (2), 271–279. doi:10.1007/s10637-014-0190-6
- Peterson, L. E. (2019). Small Molecule Docking of DNA Repair Proteins Associated with Cancer Survival Following PCNA Metagene Adjustment: A Potential Novel Class of Repair Inhibitors. *Molecules* 24 (3), 645. doi:10.3390/molecules24030645
- Petragnano, F., Pietrantoni, I., Camero, S., Codenotti, S., Milazzo, L., Vulcano, F., et al. (2020). Clinically Relevant Radioresistant Rhabdomyosarcoma Cell Lines: Functional, Molecular and Immune-Related Characterization. *J. Biomed. Sci.* 27 (1), 90. doi:10.1186/s12929-020-00683-6
- Raleigh, D. R., and Haas-Kogan, D. A. (2013). Molecular Targets and Mechanisms of Radiosensitization Using DNA Damage Response Pathways. *Future Oncol.* 9 (2), 219–233. doi:10.2217/fon.12.185
- Roeske, J. C., Nunez, L., Hoggart, M., Labay, E., and Weichselbaum, R. R. (2007). Characterization of the Theoretical Radiation Dose Enhancement from Nanoparticles. *Technol. Cancer Res. Treat.* 6 (5), 395–401. doi:10.1177/153303460700600504
- Roth, M. T., Cardin, D. B., Borazanci, E. H., Steinbach, M., Picozzi, V. J., Rosemery, A., et al. (2020). A Phase II, Single-Arm, Open-Label, Bayesian Adaptive Efficacy and Safety Study of PBI-05204 in Patients with Stage IV Metastatic Pancreatic Adenocarcinoma. *Oncologist* 25 (10), e1446–e150. doi:10.1634/theoncologist.2020-0440
- Shrivastav, M., De Haro, L. P., and Nickoloff, J. A. (2008). Regulation of DNA Double-Strand Break Repair Pathway Choice. *Cell Res.* 18 (1), 134–147. doi:10.1038/cr.2007.111
- Smith, J. A., Madden, T., Vijjeswarapu, M., and Newman, R. A. (2001). Inhibition of Export of Fibroblast Growth Factor-2 (FGF-2) from the Prostate Cancer Cell Lines PC3 and DU145 by Anvirzel and its Cardiac Glycoside Component, Oleandrin. *Biochem. Pharmacol.* 62 (4), 469–472. doi:10.1016/s0006-2952(01)00690-6
- Stupp, R., Hegi, M. E., Mason, W. P., van den Bent, M. J., Taphoorn, M. J., Janzer, R. C., et al. (2009). Effects of Radiotherapy with Concomitant and Adjuvant Temozolamide versus Radiotherapy Alone on Survival in Glioblastoma in a Randomised Phase III Study: 5-year Analysis of the EORTC-NCIC Trial. *Lancet Oncol.* 10 (5), 459–466. doi:10.1016/S1470-2045(09)70025-7
- Timme, C. R., Rath, B. H., O'Neill, J. W., Camphausen, K., and Tofilon, P. J. (2018). The DNA-PK Inhibitor VX-984 Enhances the Radiosensitivity of Glioblastoma Cells Grown In Vitro and as Orthotopic Xenografts. *Mol. Cancer Ther.* 17 (6), 1207–1216. doi:10.1158/1535-7163.MCT-17-1267
- Vlashi, E., and Pajonk, F. (2015). Cancer Stem Cells, Cancer Cell Plasticity and Radiation Therapy. *Semin. Cancer Biol.* 31, 28–35. doi:10.1016/j.semancer.2014.07.001
- Wang, H., Mu, X., He, H., and Zhang, X. D. (2018). Cancer Radiosensitizers. *Trends Pharmacol. Sci.* 39 (1), 24–48. doi:10.1016/j.tips.2017.11.003
- Wang, W. J., Long, L. M., Yang, N., Zhang, Q. Q., Ji, W. J., Zhao, J. H., et al. (2013). NVP-BEZ235, a Novel Dual PI3K/mTOR Inhibitor, Enhances the Radiosensitivity of Human Glioma Stem Cells In Vitro. *Acta Pharmacol. Sin.* 34 (5), 681–690. doi:10.1038/aps.2013.22
- Wu, W., Klockow, J. L., Zhang, M., Lafourte, F., Chang, E., Jin, L., et al. (2021). Glioblastoma Multiforme (GBM): An Overview of Current Therapies and Mechanisms of Resistance. *Pharmacol. Res.* 171, 105780. doi:10.1016/j.phrs.2021.105780

Conflict of Interest: RN and PY are consultants for Phoenix Biotechnology, Inc.

The remaining authors declare that the research was conducted in the absence of any commercial or financial relationships that could be construed as a potential conflict of interest.

Publisher's Note: All claims expressed in this article are solely those of the authors and do not necessarily represent those of their affiliated organizations, or those of the publisher, the editors and the reviewers. Any product that may be evaluated in this article, or claim that may be made by its manufacturer, is not guaranteed or endorsed by the publisher.

Copyright © 2022 Colapietro, Yang, Rossetti, Mancini, Vitale, Chakraborty, Martellucci, Marampon, Mattei, Gravina, Iorio, Newman and Festuccia. This is an open-access article distributed under the terms of the Creative Commons Attribution License (CC BY). The use, distribution or reproduction in other forums is permitted, provided the original author(s) and the copyright owner(s) are credited and that the original publication in this journal is cited, in accordance with accepted academic practice. No use, distribution or reproduction is permitted which does not comply with these terms.